

Phenomenological theory of magnetic anisotropy in thin films and multilayers

A.N. Bogdanov^{1*}, U.K. Rößler^{2#}

¹*Max-Planck-Institut für Physik komplexer Systeme
Nöthnitzer Straße 38, D-01187 Dresden, Germany*

²*Institut für Festkörper- und Werkstofforschung Dresden
Postfach 270016, D-01171 Dresden, Germany*

(November 23, 2018)

Within a phenomenological approach the density of induced uniaxial anisotropy in nanostructures $K(\mathbf{r})$ is treated as a physical field additional to the magnetization $\mathbf{M}(\mathbf{r})$. The equilibrium distributions of $K(\mathbf{r})$ are formed under the influence of the surfaces and internal interactions. The functions $K(\mathbf{r})$ and $\mathbf{M}(\mathbf{r})$ are calculated for a magnetic layer between two nonmagnetic spacers. It is shown that the transition from the phase with magnetization in plane to the perpendicular phase occurs continuously via an intermediate phase which is inhomogeneous across the layer-thickness. The theory explains experimentally observed thickness dependences of the effective anisotropy and gives a method to obtain values of the characteristic parameters for the theory from experimental data. It is shown that the separation of the induced anisotropy into volume and surface contribution is valid only for thick films.

Magnetic anisotropy is one of the key properties exploited in ferromagnetic nanostructures. Reduced dimensionality may greatly alter the effective magnetic anisotropy of such structures. For layered systems, numerous investigations demonstrate that reduced thickness and complex interactions on surfaces and interfaces induce uniaxial magnetic anisotropy which, by orders of magnitude, exceeds the values of the intrinsic anisotropy in the corresponding bulk materials [1–3]. During the last decade a large variety of magnetic thin films and multilayers have been synthesized and investigated experimentally. They have already found applications in modern magnetoelectronics such as spin-valves or magnetoresistive heads [4].

Recent first principle numerical calculations have proved the reliability of the quantum-mechanical microscopic theory in its applications to magnetic nanostructures [5,6]. They are offering considerable insight into the phenomena of induced anisotropy. However, these *ab initio* calculations are still unable to give a complete description of the magnetization structures and processes in real layered systems. Hence, our understanding of and control over the magnetic anisotropy of nanostructures is rather incomplete. Up to now, the analysis of experimental data on anisotropy effects in magnetic layered systems is mostly based on the effective volume anisotropy method introduced by Néel about fifty years ago [7]. Within this approach the value of average induced uniaxial anisotropy in a magnetic layer of thickness d is given by an empirical ansatz

$$K_{\text{eff}} = K_V + \frac{K_S}{d} \quad (1)$$

where K_V is the volume anisotropy (per unit volume), and K_S is the surface (interface) contribution (per unit area). For many layered systems with reduced thickness, the function $K(1/d)$ becomes strongly nonlinear which is at variance with eq. (1) [1,2,8–11]. Moreover, the general validity of the Néel theory has been questioned in a number of publications [1,12]. The separation of the uniaxial anisotropy into volume and surface contribution and the reduction of surface anisotropy into an effective volume contribution should be considered as an excessive simplification. Furthermore, equation (1) implies that the anisotropy is constant within a magnetic layer and, thus, stabilizes a homogeneous distribution of the magnetization. It was shown, however, that the competition between volume and surface anisotropies may induce inhomogeneous states in magnetic films and multilayer structures [13]. The surface induced anisotropy can also gradually relax into the depth of the layer [14]. On the whole, the heuristic Néel approach as well as similar models have succeeded to give qualitative explanations of some general features of the induced anisotropy. However, they do not account for many other observed effects and they fail to give a quantitative description of the magnetization structures in magnetic nanostructures.

In this paper we propose a simple phenomenological theory which gives a consistent method to calculate the anisotropy and the equilibrium magnetization in thin films and multilayers. Let us consider a magnetic nanostructure embedded into nonmagnetic media. It may be a thin magnetic film confined by the interface with the substrate and the surface, or a magnetic layer between nonmagnetic spacers in a multilayer, or any other magnetic inclusion in a nonmagnetic matrix (such as nanowires, magnetic dots, or magnetic clusters). The magnetic energy of such a nanostructure can be written as an integral over its volume

$$W_m = \int \left[A \sum_i \left(\frac{\partial \mathbf{m}}{\partial x_i} \right)^2 + K(\mathbf{r})(\mathbf{m} \cdot \mathbf{n})^2 - \mathbf{H} \cdot \mathbf{M} - \frac{1}{2} \mathbf{H}_d \cdot \mathbf{M} \right] d\mathbf{r}. \quad (2)$$

Here $\mathbf{m} = \mathbf{M}/M_0$ is the normalized value of the magnetization vector \mathbf{M} ($M_0 = |\mathbf{M}|$), \mathbf{n} is a unity vector perpendicular to the surface of the layer, A is the exchange stiffness constant, \mathbf{H} is an external magnetic field, and \mathbf{H}_d is a demagnetizing field. The second term in (2) is the energy density of the induced uniaxial anisotropy. To describe the distribution of $K(\mathbf{r})$ within the nanostructure we introduce an interaction functional of Landau-Ginzburg type

$$W_A = \int \left[\alpha \sum_i \left(\frac{\partial K}{\partial x_i} \right)^2 + f(K) \right] d\mathbf{r}. \quad (3)$$

The first term in (2) represents the stiffness energy and $f(K)$ is the energy of a homogeneous induced anisotropy. In many cases the function $f(K)$ may be written as $f(K) = aK^2 + 2bK$. The stiffness parameter $\alpha > 0$ together with $a > 0$ characterize the resistance of the system against the uniaxial anisotropy imposed by the boundaries. The linear term in $f(K)$ reflects the tendency for symmetry breaking and the ensuing rise of homogeneous uniaxial anisotropy. Minimization of $f(K)$ yields the value of this anisotropy $K_b = -b/a$. The scalar function $K(\mathbf{r})$ may be treated as a physical field additional to the magnetization field $\mathbf{M}(\mathbf{r})$. Both fields are coupled by the anisotropy energy in (2). In most cases, this coupling energy should be negligible compared to the strong surface and volume interactions inducing the uniaxial anisotropy. Thus, the equilibrium distribution $K(\mathbf{r})$ can be calculated independently from the magnetization field by minimization of the functional (3). The anisotropy on the confining surfaces is supposed to have values $K(\mathbf{r})_S = K_0$ fixing the boundary conditions for the variation problem. Then, the equilibrium distributions of the magnetization are determined by variation of the functional (2) with this definite function $K(\mathbf{r})$. Here, the boundary conditions K_0 are kept constant. But, in general, K_0 may vary within the surfaces, and all phenomenological constants in (3) may depend on characteristic sizes of the nanostructure. The values K_0 (volume anisotropy density on the surfaces) should not be confused with the ‘‘surface anisotropy’’ K_S in (1) which is an anisotropy energy per area. The relation between these quantities will be discussed below.

As an application of the theory we calculate the induced anisotropy and the magnetization in a magnetic layer of thickness d sandwiched between two identical nonmagnetic spacers. The layer is supposed to be infinite in x and y directions and bounded by parallel planar surfaces $z = \pm d/2$. On the surfaces the anisotropy is $K(d/2) = K(-d/2) = K_0$. The vector \mathbf{n} is directed along the z -axis and $K_0 > 0$ (perpendicular, surface induced anisotropy). Within the magnetic plate $K(\mathbf{r})$ varies along z -direction and is homogeneous in (x, y) plane. Variation of the functional (3) yields the following solution for $K(z)$:

$$K(z) = K_b + \frac{(K_0 - K_b) \cosh(z/\lambda_a)}{\cosh(d/(2\lambda_a))} \quad (4)$$

where $\lambda_a = \sqrt{\alpha/a}$ is a characteristic length. To derive the equilibrium functions $\mathbf{M}(\mathbf{r})$ one has to minimize the functional for the magnetic energy (2) with $K(z)$ given by (4). We consider structures that are homogeneous in the plate plane (i.e. monodomain structures). Further, we ignore the variation of M_0 observed in some multilayers [15]. Under these assumptions the magnetization in the layer is described by the polar angle $\theta(z)$ between the vector \mathbf{M} and z -axis. For such a one-dimensional problem the magnetostatic equations for \mathbf{H}_d have a rigorous solution, and the corresponding stray field energy is expressed by an anisotropy-like term $w_d = -\mathbf{H}_d \mathbf{M}/2 = 2\pi M_0^2 \cos^2(\theta)$ [16]. This energy contribution is commonly named ‘‘shape anisotropy’’. Thus, the functional (2) with $K(z)$ given by (4) may be expressed in the following reduced form

$$W = 2\pi M_0^2 \int_{-d/2}^{d/2} \left\{ \lambda_{ex}^2 \left(\frac{d\theta}{dz} \right)^2 - \frac{\tilde{K}(z)}{2\pi M_0^2} \cos^2 \theta - h \cos(\theta - \psi) \right\} dz \quad (5)$$

where $h = H/(2\pi M_0)$ is a reduced value of the magnetic field and ψ is the angle between the vector \mathbf{H} and z -axis, $\lambda_{ex} = \sqrt{A/(2\pi M_0^2)}$ is the exchange length, and the volume density of the total anisotropy $\tilde{K}(z)$ is

$$\tilde{K}(z) = -2\pi M_0^2 + \frac{K_0 \cosh(z/\lambda_a)}{\cosh(d/(2\lambda_a))}. \quad (6)$$

For simplicity we suppose that the homogeneous part of the induced anisotropy K_b (see (4)) is included into the coefficients K_0 and $2\pi M_0^2$.

The energy (5) has the functional form of an uniaxial ferromagnet with anisotropy $\tilde{K}(z)$ (6) varying along the layer thickness. The distribution of $\tilde{K}(z)$ within the layer strongly depends on the layer thickness (Fig. 1). The length λ_a

characterizes the extension of the surface anisotropy into the layer depth and may be named “*penetration depth of the induced anisotropy*”. When $d \gg \lambda_a$ the induced anisotropy is localized near surfaces and rapidly relaxes into the depth of the layer. For thinner layers, where λ_a and d have the same order of magnitude, the induced anisotropy attains considerable values within all the layer (Fig. 1). The possible magnetic phases and the regions of their stability are determined by optimization of the energy (5) with free boundary conditions that read for this case $(d\theta/dz)|_{z=\pm d/2} = 0$. A complete analysis of the functional (5) will be done elsewhere. Here we only discuss some general properties of the solutions at zero field as representative for the problem. In this case the layer thickness d and the parameters $q = K_0/(2\pi M_0^2)$ and $\Lambda = \lambda_{ex}/\lambda_a$ span the phase space of the solutions. A typical (q, d) phase diagram for fixed values of Λ is shown in Fig. 2. It consists of two regions where homogeneous phases exist with either *perpendicular* ($\theta = 0$) or *parallel* ($\theta = \pi/2$) magnetization. These are separated by an inhomogeneous (*twisted*) phase where the angle θ gradually increases from a definite value $\theta_1 \geq 0$ on the surfaces to a largest value in the center $\theta_1 < \theta_2 \leq \pi/2$.

The perpendicular phase is stable for small values of the thickness and when $q > 1$. The parallel phase exists only in rather thick layers and when the parameter q is smaller than a critical value $q_c(\Lambda)$. In the region $q > q_c$ the perpendicular phase transforms continuously into the twisted phase at the critical line $d_1(q)$. For $1 < q < q_c$ the region of the existence of the twisted phase is bound by two lines of second order transitions into the homogeneous phases $d_1(q)$ and $d_2(q)$. Thus, according to our model the transition between the parallel and the perpendicular phases always occurs continuously via the transformation into an intermediary (twisted) phase. Fig. 3 shows the evolution of the magnetic structures during such a transition.

By integrating $\tilde{K}(z)$ in (6) over z one obtains for the average value of the uniaxial anisotropy density

$$K_{\text{eff}} = \frac{1}{d} \int_{-d/2}^{d/2} \tilde{K}(z) dz = -2\pi M_0^2 + \frac{K_0 \tanh(d/(2\lambda_a))}{d/(2\lambda_a)}. \quad (7)$$

Values of the anisotropy K_{eff} have been measured in many layered systems [1,2]. Usually, experimental values of K_{eff} are plotted as product $K_{\text{eff}}d$ versus d . In Fig. 4 the thickness dependence of the function $\Phi(d) = K_{\text{eff}}d$ corresponding to (7) is shown for different values q .

In the limit of large thickness ($d \gg \lambda_a$) the functions $\Phi(d)$ are negative and depend linearly on the thickness (with slope equal to the value of the shape anisotropy). In thinner layers ($d \leq \lambda_a$) the functions $\Phi(d)$ become nonlinear. For $q < 1$ they are always negative (parallel anisotropy) and reach zero as the thickness decreases to zero. For $q > 1$, the function $\Phi(d)$ changes sign at the critical thickness d_0 determined by the equation

$$K_0 \tanh\left(\frac{d_0}{2\lambda_a}\right) = \frac{2\pi M_0^2 d_0}{2\lambda_a} \quad (8)$$

and remains positive for $0 < d < d_0$ manifesting the existence of the perpendicular anisotropy in this region. The function $\Phi(d)$ reaches the maximum value for the thickness

$$d_{\text{max}} = 2\lambda_a \text{arc cosh} \sqrt{\frac{K_0}{2\pi M_0^2}}, \quad (9)$$

and then monotonically decreases to zero as $d \rightarrow 0$ (Fig. 4). Experimentally obtained functions $\Phi(d)$ are in close accordance with our theoretical results. E.g., nonmonotonic dependencies of $\Phi(d)$ have been observed for Co/Au multilayers [14], Co/Ir multilayers [8], or for Ni/Cu multilayers and Cu/Ni/Cu sandwiches [9–11]. Taking experimental values for d_0 and d_{max} it is possible to calculate the parameters q and λ_a from eqs. (8) and (9). E.g., for Co/Au [14] films this yields $q = 4.6$ and $\lambda_a = 1.9\text{\AA}$. For Ni/Cu multilayer systems the function $\Phi(d)$ in the regions of perpendicular anisotropy has been obtained by three different experimental methods [9–11]. The results from these experiments show similar functional dependencies for $\Phi(d)$. However, the measured values display considerable quantitative differences. Taking the experimental data from [9] and [10] we derive the following values for the characteristic parameters $q = 2.1$ and 2.2 , $\lambda_a = 26.4\text{\AA}$ and 31.9\AA . In contrast to the full curves from our theory in Fig. 4 experimental dependencies $\Phi(d)$ for these Ni-films become negative again for finite values of the thickness manifesting the reentrance of planar anisotropy in ultrathin films [9–11]. It should be noted in this respect that for the calculation of $\Phi(d)$ (Fig. 4) the phenomenological parameters K_0 are kept constant in this simple approach. According to experimental observations they may depend on the layer thickness, and they may be sensitive to details of the film preparation, e.g. via surface reconstructions, misfit strain or misfit dislocations etc. In particular, it was established experimentally that in the Ni-films under discussion surface anisotropy decreases with decrease of the layer thickness due to magnetoelastic interactions [17]. For decreasing values of K_0 the theoretical dependencies $\Phi(d)$ become negative in the limit of very thin films (dashed line in Fig. 4). This thickness dependency of the phenomenological parameters K_0 as well as other

phenomenological constants should be considered by introducing appropriate models in future work based on further experimental results and results from *ab initio* calculations.

The distribution of the induced anisotropy and the magnetization in a magnetic layer can also be investigated within a discretized model which is useful in the limit of ultrathin layers or for comparison with *ab initio* calculations. In this case the equilibrium values of the induced anisotropy in the magnetic layer consisting of N magnetic planes are determined by minimization of the energy

$$\widetilde{W}_A = \sum_{n=1}^{N-1} \left[\left(1 + \frac{2\lambda_a^2}{\Delta^2} \right) K_n^2 - \frac{2\lambda_a^2}{\Delta^2} K_n K_{n+1} + \frac{2b}{a} K_n \right] \Delta \quad (10)$$

where Δ is the distance between two adjacent planes. Equilibrium profiles of K_n for symmetric boundary conditions $K_1 = K_N = K_0$ are shown in Fig. 5. Using these profiles, the orientation of the magnetization vectors in the planes θ_n can be calculated by minimization of the discretized analogue of the energy (5). The characteristic functions for the discretized model $\Phi_N = -2\pi M_0^2 N \Delta + \sum_{n=1}^N K_n$ shown in Fig. 6 display the same dependence on thickness $d = N \Delta$ as the continuous model (Fig. 4).

Finally, we discuss the relation between our theory and the traditional approach. For large thickness ($d \gg \lambda_a$), the function (4) may be asymptotically written as

$$K(z) = K_0 \exp\left(-\frac{d - |z|}{\lambda_a}\right). \quad (11)$$

The function $K(z)$ has finite values only in the vicinity of the surfaces and equals zero in the main part of the layer. Integrating (11) with respect to z yields the anisotropy energy (per area)

$$K_s = K_0 \int_0^\infty \exp(-\xi/\lambda_a) d\xi = K_0 \lambda_a. \quad (12)$$

The integral parameter K_s is equal to the additional energy connected with surface induced anisotropy. Similar parameters characterize surface tension in liquids and domain wall energy in the theory of magnetic domains. Expanding K_{eff} in (7) for large d/λ_a and substituting for K_s (12) one obtains the Néel anisotropy ansatz (1). In the region of large thickness the surface anisotropy may be transformed into a surface term which should be included into the boundary conditions of the corresponding variation problem for the magnetization. For this case the calculation of the magnetization in magnetic layers firstly has been done by Thiaville and Fert [13]. It is clear that the surface anisotropy K_s is meaningful only in the case of a strong confinement of the induced anisotropy to the surface, i.e. when $d \gg \lambda_a$. This relation determines the region of the validity for the Néel approach and other approaches that reduce surface effects to an effective surface energy contribution. Beyond this region the function $\tilde{K}(z)$ of eq. (6) has finite values within all the layer and the separation of the induced anisotropy into a surface and a volume contribution becomes meaningless.

In conclusion, our theory considers inhomogeneous distributions of induced magnetic anisotropy. It is able to describe many of the experimental features found for thin ferromagnetic films. In particular, the nonlinear deviations from Néel's approach for surface anisotropy found in various experiments are consistently explained.

We thank H. Eschrig, R. Hayn, K.-H. Müller, and P.M. Oppeneer for discussion. A.N.B. thanks P. Fulde for hospitality and support. U.K.R. is supported by DFG.

* Permanent address: Donetsk Institute for Physics and Technology, 340114 Donetsk, Ukraine; e-mail: bogdanov@kinetic.ac.donetsk.ua

Corresponding author; e-mail: u.roessler@ifw-dresden.de

- [1] W. J. M. de Jonge, P. J. H. Bloemen, and F. J. A. den Broeder, in *Ultrathin Magnetic Structures* vol. I edited by J. A. C. Bland, B. Heinrich, (Springer-Verlag, Berlin 1994) p. 65.
- [2] M.T. Johnson, *et al.*, Rep. Prog. Phys. **59** (1996) 1409.
- [3] P. Pouloupoulos and K. Baberschke, J. Phys: Cond. Matter **11** (1999) 9495.
- [4] F. J. Himpsel, *et al.*, Adv. Phys. **47** (1998) 511.
- [5] G. Y. Guo, J. Magn. Magn. Mater. **176** (1997) 97.
- [6] P. Weinberger, L. Szunyogh, Comp. Mat. Sc. **17** (2000) 414.
- [7] L. Néel, J. Physique Radium **15** (1954) 225.

- [8] F. J. A. den Broeder, W. Hoving, P. J. H. Bloemen, *J. Magn. Magn. Mater.* **93** (1991) 562.
- [9] R. Jungblut, *et al.*, *J. Appl. Phys.* **75** (1994) 6424.
- [10] G. Bochi, *et al.*, *Phys. Rev. B* **53** (1996) 1729.
- [11] K. Ha and R. C. O'Handley, *J. Appl. Phys.* **87** (2000) 5944.
- [12] G.T. Rado, *J. Magn. Magn. Mater.* **104-107** (1992) 1679.
- [13] A. Thiaville and A. Fert, *J. Magn. Magn. Mater.* **113** (1992) 161.
- [14] T. Kingetsu and K. Sakai, *Phys. Rev. B* **48** (1993) 4140.
- [15] F. Wilhelm, *et al.*, *Phys. Rev. Lett.* **85** (2000) 413.
- [16] A. Hubert, R. Schäfer, *Magnetic Domains* (Springer-Verlag, Berlin 1998) p. 696.
- [17] G. Bochi, *et al.*, *Phys. Rev. B* **52** (1995) 7311.

FIG. 1. Inhomogeneous distribution of the anisotropy $\tilde{K}(z)$ across a magnetic film according to eq. (6). For the curves from the top to the bottom, the chosen value of λ_a decreases.

FIG. 2. Typical phase diagram (schematic) for the magnetization structure of magnetic films described by eqs. (5) and (6) for fixed $\Lambda = \lambda_{ex}/\lambda_a$ and in zero field. Depending on layer thickness d and on the strength of induced uniaxial anisotropy at the film boundaries $q \sim K_0$ three phases may exist as symbolically depicted by the insets. A twisted phase is separated from the two homogeneous phases by second-order transition lines d_1 and d_2 . At the dashed line the energy for perpendicular and parallel phase would be equal. For $q > q_c$ only perpendicular and twisted phase exist.

FIG. 3. Magnetization distribution across magnetic films for fixed q with increasing thickness d . Transition from perpendicular to twisted structure at d_1 and from twisted to parallel at d_2 .

FIG. 4. Characteristic function $\Phi(d) = K_{\text{eff}} d$ showing the dependence of the effective magnetic anisotropy eq. (7) on film thickness. Full lines give the typical behaviour when the anisotropy K_0 at the boundaries is fixed. The dashed line shows reentrance of the parallel magnetization when K_0 decreases with decreasing d in the case with $q > 1$.

FIG. 5. Distribution of local anisotropy for the discretized model eq. (10) with various N and fixed thickness.

FIG. 6. Examples of characteristic functions for the effective anisotropy of the discretized model. Symmetric boundary conditions $K_0=0.05$ (\square), $K_0=1$ (\bullet) and $\lambda_a^2 = 10$, $b = 0.5$, $a = \Delta = 1$, $M_0 = 0.2$.

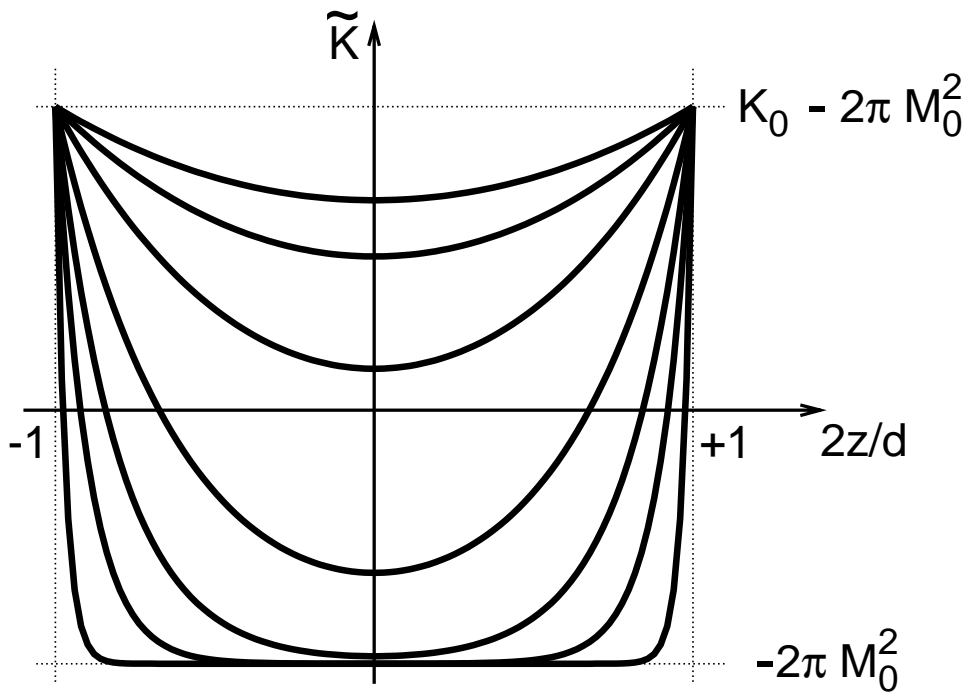


Fig. 1
 A.N. Bogdanov
 Phenomenological theory of magnetic anisotropy ...

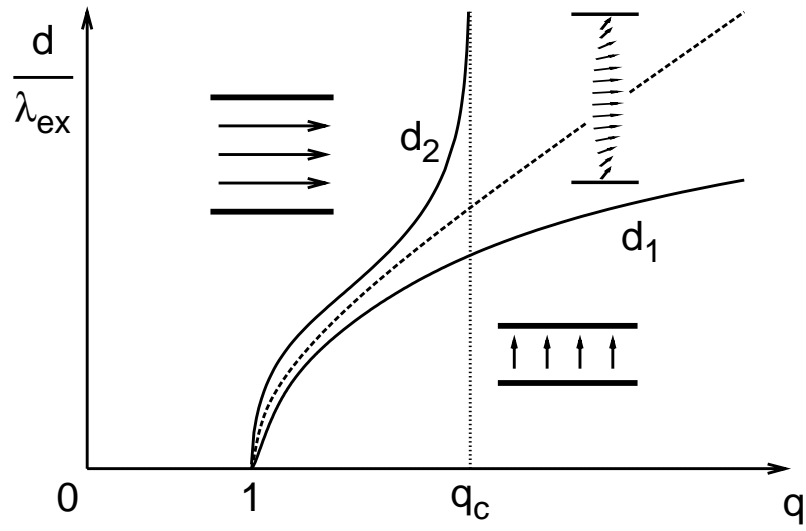


Fig. 2
 A.N. Bogdanov
 Phenomenological theory of magnetic anisotropy ...

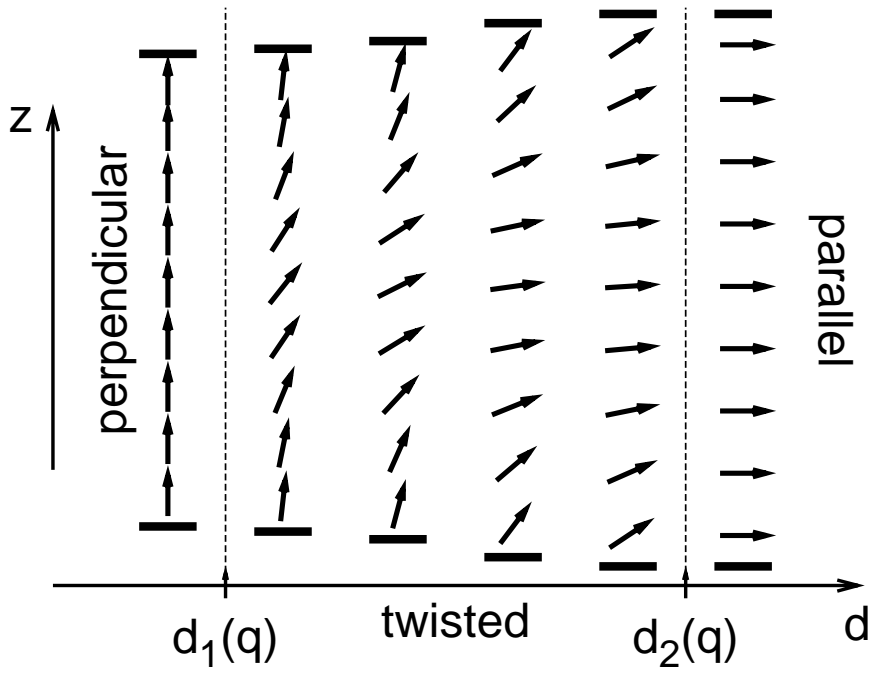


Fig. 3
 A.N. Bogdanov
 Phenomenological theory of magnetic anisotropy ...

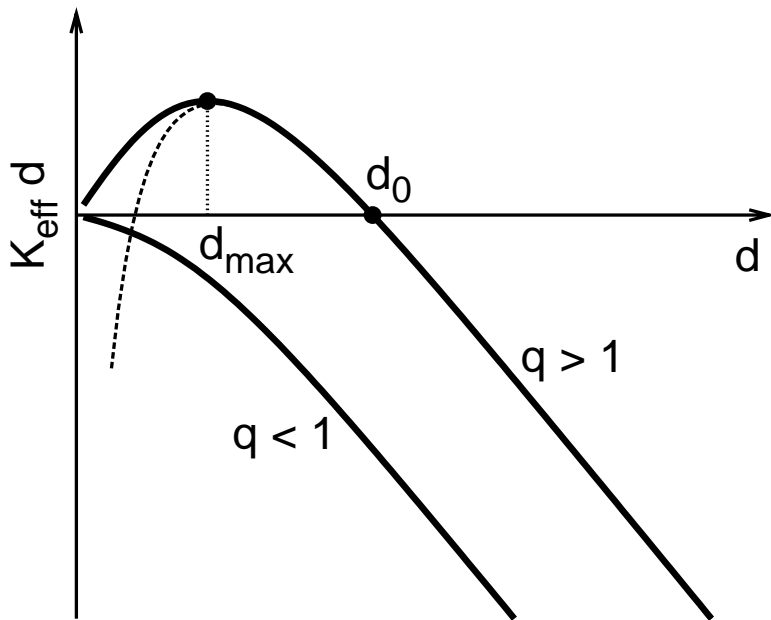


Fig. 4
 A.N. Bogdanov
 Phenomenological theory of magnetic anisotropy ...

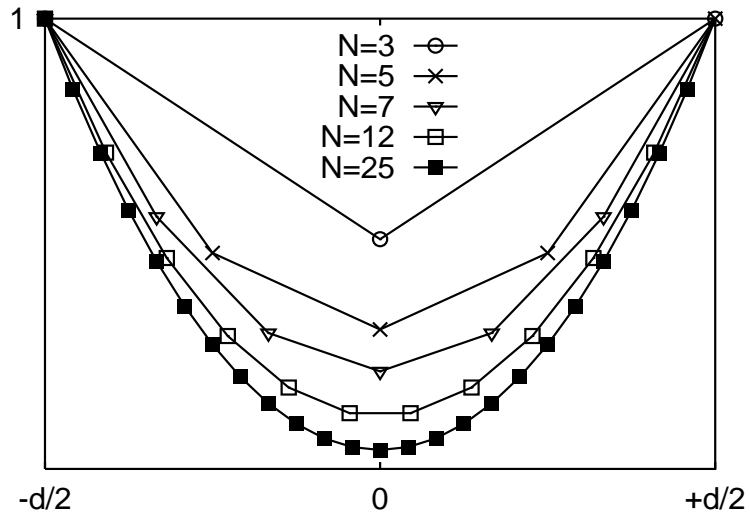


Fig. 5
 A.N. Bogdanov
 Phenomenological theory of magnetic anisotropy ...

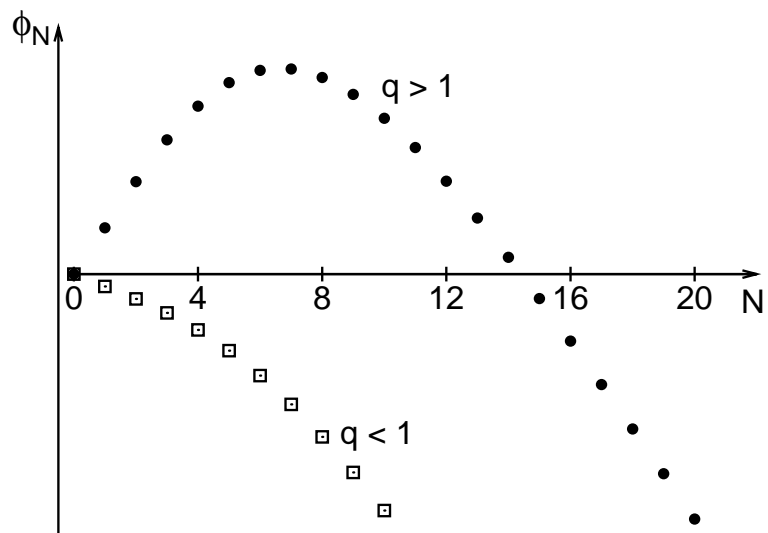


Fig. 6
 A.N. Bogdanov
 Phenomenological theory of magnetic anisotropy ...